

# Hopping and Jumping between Potential Energy Surfaces<sup>†</sup>

E. J. Heller,<sup>\*,‡</sup> Bilha Segev,<sup>\*,§</sup> and A. V. Sergeev<sup>§</sup>

Departments of Chemistry and Physics, Harvard University, Cambridge, Massachusetts 02138, and  
Department of Chemistry, Ben-Gurion University of the Negev, POB 653, Beer-Sheva 84105, Israel

Received: May 2, 2002; In Final Form: June 4, 2002

Novel approaches to surface hopping (in the case in which surfaces cross in classically allowed regions) and surface “jumping” (in cases in which they never cross or they cross in classically forbidden regions) are discussed. Classically forbidden transitions necessarily involve discontinuous “jumps” in position or momentum or both (but so as to preserve energy). In general, the jumps are discontinuous changes in nuclear positions or momenta on the time scale of the electronic transition. After reviewing various approaches in one dimension, a phase-space approach is applied to multidimensional systems with large energy gaps, in which the traditional semiclassical approaches are more difficult to apply. The concept of jumps extends the spirit of surface hopping into new regimes.

## 1. Introduction

The crossing of potential energy surfaces (and the flow of nuclear wave function amplitudes between them) becomes important in many different contexts in chemical physics. Photochemical processes often involve dynamics on surfaces that cross (or can be made to cross in an appropriate diabatic representation). Photophysical processes involving radiationless transitions between different Born–Oppenheimer potential energy surfaces are extremely common. Finally, once we “dress” an initial potential energy surface with the energy of a photon, radiative processes involving absorption or emission of a photon are also seen to involve transitions between crossing or close-lying potential energy surfaces.

Some years ago, Tully and Preston<sup>1</sup> introduced an approach for approximate treatment of dynamics at regions of close-lying potential energy surfaces. In many subsequent trials and refinements, it has proved a worthy computational tool, simple to implement and also very intuitive. The “surface hopping” method has its roots in the Landau–Zener theory<sup>2</sup> but goes beyond it in dealing with multiple crossings and with many degrees of freedom.

Related theories include the exponential energy gap law of radiationless transitions<sup>3</sup> and the exponential momentum gap law of Ewing<sup>4</sup> for vibrational predissociation (in which a high-frequency vibrational mode plays the role of the electronic state, relative to a low-frequency van der Waals mode). In these studies, considerable effort has been devoted to developing new intuition for nonclassical Franck–Condon factors. The emphasis has been on the mode competition problem and the overall dependence of rates on the energy or quantum number gaps. Our emphasis is instead directly on the features of the potential energy surfaces, which control the Franck–Condon factors, which in turn control the rates.

The fundamental idea that permits a classical treatment of surface hopping is contained in the Landau–Zener–Stuckelberg model,<sup>2</sup> which shows that the hops from one surface to another

are localized to the region where the surfaces cross or almost cross. For weak coupling, the probability for hopping is given in terms of the overall coupling,  $W$ , between the surfaces, the difference in slopes,  $|\Delta\mathbf{F}_\perp|$ , normal to the intersection of the two potentials at the crossing, and the speed,  $p_\perp/m$ , with which the trajectory goes through the crossing region:

$$P = k\tau = \frac{2\pi W^2}{\hbar^2 \delta E} \frac{1}{p_\perp} \left[ \frac{m\hbar \delta E}{|\Delta\mathbf{F}_\perp|} \right] \\ = \frac{2\pi W^2}{\hbar} \left[ \frac{m}{p_\perp |\Delta\mathbf{F}_\perp|} \right] \quad (1)$$

In this paper, we study hopping and jumping between potential energy surfaces. In section 2, eq 1 for the Landau–Zener–Stuckelberg rate is rederived following Bergsma et al.<sup>5</sup> In the weak-coupling regime, transitions between potential energy surfaces are controlled by Franck–Condon matrix elements. The relation between these matrix elements (overlap integrals) and the hopping or jumping mechanism is the subject of the paper. In section 3, within the traditional semiclassical perspective, the transition is shown to occur through a small hop or a large jump to the point in coordinate space where the two surfaces cross,  $x_c$ . In general,  $x_c$  defined in this way is complex. A likewise complex momentum is then associated with this jump. Finding it is easy in one dimension but much more complicated in the multidimensional case. In section 4, the same Franck–Condon integrals are considered in the Wigner representation. This time, the point that dominates the Franck–Condon factor is real. The phase-space formulation is applicable for any dimension. A relation between the jumping point ( $x_m$ ,  $p_m$ ) in real phase space and the complex surface-crossing coordinate,  $x_c$ , and momentum,  $p_c$ , in the one-dimensional case is suggested and demonstrated for model systems, in limiting cases and through numerical examples in sections 4 and 5, respectively. Section 6 presents conclusions.

## 2. Trajectory Binning Method

Some years ago, Bergsma et al.<sup>5</sup> introduced a simple way to evaluate the hopping probability by a somewhat different stochastic approach. We call it proximity hopping.

<sup>†</sup> Part of the special issue “John C. Tully Festschrift”.

<sup>\*</sup> To whom correspondence should be addressed. E-mail addresses: heller@physics.harvard.edu and bsegev@bgumail.bgu.ac.il.

<sup>‡</sup> Harvard University.

<sup>§</sup> Ben-Gurion University of the Negev.

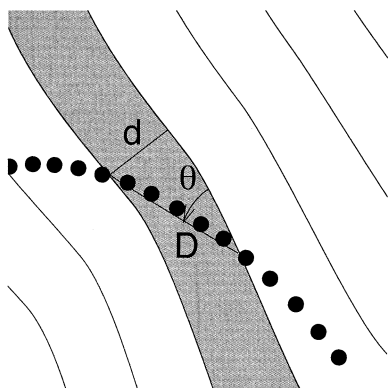


**Figure 1.** Contours of the difference potential and a trajectory at equal time steps.

The idea is as follows. For a given trajectory, we monitor the energy difference between the two potential energy surfaces at the location of the trajectory. If this energy difference becomes less than some specified amount,  $\delta E$ , the trajectory is subjected to hopping at a fixed probability  $\phi$  per unit time. This is easy to arrange by taking  $\phi$  to be, say, 0.05 per time step. The overall rate of hopping is governed by  $\delta E$  and  $\phi$ , but the local hopping rate is correctly governed by the above Ansatz. We now proceed to demonstrate this.

Consider Figure 1, which shows a contour plot of  $V_A(\mathbf{r}^N) - V_B(\mathbf{r}^N)$  for a two-dimensional case, together with a particular trajectory on the  $V_A$  potential surface. This trajectory is plotted as dots spaced at equal times, which could be the sample times used to inquire whether the trajectory is in the hopping energy range. The space between a pair of contour lines corresponds to an energy range

$$-\frac{\delta E}{2} \leq E \leq \frac{\delta E}{2} \quad (2)$$

The amount of time spent between the two shaded contour lines is proportional to the contribution that this particular trajectory segment will make to the hopping rate. The time  $\tau$  spent between contours is the distance  $D$  traversed divided by the velocity or

$$\tau = \frac{D}{(p/m)} = \frac{md}{p \sin \theta} = \frac{md}{p \sin p_{\perp}} \quad (3)$$

in which  $p$  is the magnitude of the momentum,  $p_{\perp} = p \sin \theta$  is the magnitude of the momentum perpendicular to the contour lines, and  $m$  is the mass. The perpendicular separation  $d$  between the contours is

$$d = \frac{\delta E}{|\Delta \mathbf{F}_{\perp}|} \quad (4)$$

where

$$|\Delta \mathbf{F}_{\perp}| = |\nabla V_A(\mathbf{r}^N) - \nabla V_B(\mathbf{r}^N)| \quad (5)$$

evaluated in the vicinity of the crossing region.  $\Delta \mathbf{F}_{\perp}$  is the force change between the final and initial potential surfaces perpendicular to the contour lines of  $V_A - V_B$  at the intersection  $V_B + \hbar\omega_m = V_A$ . Taking the rate of crossing per unit time from the initial to the final surface to be

$$k = \frac{2\pi W^2}{\delta E} \quad (6)$$

in which  $W$  is a coupling parameter, the total probability  $P$  of

crossing from the initial to the final surface while on the trajectory in the region of the bin is given by eq 1. Nothing essential depends on our assumption of two degrees of freedom. Equation 1 is applicable to many degrees of freedom.

Equation 1 is the Landau–Zener–Stuckelberg rate for radiationless transition surface crossing<sup>2</sup> in the case of diabatic surfaces that intersect with small coupling  $W$ . (The adiabatic crossing probability would be  $1 - P$ .) The “proximity hopping” method may be restricted to the weak coupling limit, when  $P$  is small per encounter with a crossing. It has the advantage of making clear the origin of the role of the velocity, the angle of approach to the surface intersection, and the difference in the magnitudes of the slopes of the two potential energy surfaces. These are all purely geometric factors, which simply determine how much time the trajectories spend “exposed” to the possibility of hopping between the surfaces. In the limit where  $P$  is small, the hopping probability is related to perturbation theory, in particular, a Franck–Condon matrix element.

### 3. The Traditional Semiclassical Perspective

**3.1. Hopping at a Classically Allowed Crossing Point.** The semiclassical eigenstates may be represented as a sum of terms of the form (ignoring Maslov phases)

$$\psi(x) \approx \frac{1}{|p(x)|^{1/2}} \exp\left[-\frac{i}{\hbar} \int^x p(x') dx'\right] \quad (7)$$

A Franck–Condon overlap between two such states, each on its own Born–Oppenheimer potential energy surface, is given by

$$\langle \psi^{(A)} | \psi^{(D)} \rangle \approx \int \frac{1}{|p_A(x)|^{1/2} |p_D(x)|^{1/2}} \exp\left[\frac{i}{\hbar} \int^x p_A(x') dx' - \frac{i}{\hbar} \int^x p_D(x') dx'\right] dx \quad (8)$$

The stationary-phase evaluation of this integral requires

$$\frac{d}{dx} \left( \int^x p_A(x') dx' - \int^x p_D(x') dx' \right) = 0 \quad (9)$$

and the stationary-phase point is  $x_c$  satisfying

$$p_A(x_c) = p_D(x_c) \quad (10)$$

which implies that, because the total energy is the same on both potential energy surfaces,

$$V_A(x_c) = V_D(x_c) \quad (11)$$

This is the well-known result that the semiclassical contribution arises where potential energy surfaces cross. There may of course be more than one stationary-phase point; in what follows, we shall assume that we are dealing with the dominant contribution.

Apart from phases and an overall factor, stationary-phase evaluation of the integral gives

$$f_{A,D} = |\langle \psi_A | \psi_D \rangle|^2 \approx \sum \left| \frac{\partial(p_A - p_D)}{\partial x} \frac{1}{p_A p_D} \right|_{x=x_c} \approx \frac{1}{p(x_c) \Delta F(x_c)} \quad (12)$$

which is the one-dimensional version of eq 1.

**3.2. Generalized Crossings.** What if there is no crossing at classically allowed values of  $x$ ? There are two possibilities for

a crossing in the nonclassical regime. If it occurs at a real (but classically inaccessible) value of  $x_c$ , then the momentum at the crossing,  $p_A(x_c) = p_D(x_c)$ , is purely imaginary. (Real momentum and real position correspond to the classical regime in which only “hopping” is required). We assign the name “position jump” to label the real quantity, that is, the position, that changes in the transition. From the coordinate space perspective, the contribution to the integral is coming from overlapping tails of the wave functions. Both  $p_A(x_c)$  and  $p_A(x_c)^*$  are stationary-phase points, but one of them corresponds to exponentially increasing wave function and is discarded.

One might retain the idea of a hop that simply occurs at the forbidden crossing, but from the perspective of the classical regime, this is a finite jump to a new location. More importantly, in many dimensions, the jumping idea turns out to be quite tractable, while the stationary-phase evaluation become extremely difficult. Thus, the “complex intersection” idea will give way to another type of evaluation of the integral, wherein it is noticed that the accepting states are much higher in vibrational energy than the donor, making a great simplification possible.

It often happens that the two real potential surfaces do not cross, not even at classically forbidden regions. If one analytically continues the potentials into the complex coordinate space, the crossing (i.e., the stationary-phase point) is then at complex values of  $x$ . The momentum is generally also complex (and not purely imaginary). One finds in these cases that the position of the crossing is sometimes *mostly* imaginary and the corresponding momentum mostly real, giving a jump that is largely in momentum. If the crossing happens at  $p = p_c$ , from the form of the Hamiltonian it also must occur for opposite sign  $p = -p_c$ . For purely imaginary momentum, this is the same as  $p_c^*$ , but generally there are four stationary-phase momenta. Two give rise to increasing rather than decreasing wave functions in the classically forbidden region and are discarded, leaving two remaining. There may be constructive or destructive interference between these distinct but equal magnitude stationary-phase amplitudes. This fact was noted by Medvedev<sup>6</sup> and separately by Hunt and Child.<sup>7</sup>

Given two potential energy surfaces, it is possible to infer the propensity (as a function of the energy gap) for position versus momentum tunneling or jumping using eq 11. This is a very direct and convenient tool.

Objections might be raised to the representation of the vibrational state of the upper Born–Oppenheimer surface by a semiclassical form, because we often take it to be the ground state, which is seemingly a dubious candidate for semiclassical approximation. At a very simple level, we may note that we are using the semiclassical form only in the classically forbidden region and normally deeply within it. As pointed out long ago by Miller,<sup>8</sup> semiclassical approximations should work well in the deep tunneling regime.

In the classically forbidden region, eqs 7–11 hold yet with complex momenta and real exponents. Here, a bound wave function of the Hamiltonian,  $H(x,p)$ , with energy  $E$  in the limit of small  $\hbar$  is

$$\psi(x) \approx \exp\left(-\frac{1}{\hbar}\sigma(x)\right) \quad (13)$$

where  $\sigma(x) = S(x)/i$  and  $S(x)$  is the solution of the Hamilton–Jacobi equation

$$H(x, \partial S(x)/\partial x) = E \quad (14)$$

for which  $S(x)/i$  tends to infinity as  $|x| \rightarrow \infty$ . As long as one

considers only the classically forbidden region, the wave function (eq 13) is just one of the primitive WKB functions with a real decaying exponent and not a linear combination with complex-valued exponents (because we have omitted an unphysical exponentially increasing solution).

We define  $w$  proportional to the logarithm of the Franck–Condon factor squared so that

$$f_{A,D} = |\langle \psi_A | \psi_D \rangle|^2 \approx \exp(-2w/\hbar) \quad (15)$$

We will now proceed to find  $w$  by expanding around the complex crossing point of the initial and final potentials.

**3.3. Transitions between Bound States.** Below, we derive some general formulas for transitions between two bound states that will be needed in what follows. We suppose that the donor state is the ground vibrational state of the initial potential energy surface. We perform the integration with the quasiclassical wave functions; the dominant contribution comes from the crossing point.

Let  $V^{(D)}$  and  $V^{(A)}$  be the potentials of the donor and the acceptor Born–Oppenheimer surfaces, respectively. In the following, we use mass-weighted coordinates. We make additional assumptions regarding the functions  $V^{(D)}(x)$  and  $V^{(A)}(x)$ . For the initial potential, we assume that

$$V^{(D)}(x) = v(x - x_0) \quad (16)$$

which increases monotonically away from its minimum at  $\xi = 0$ . We assume the final potential  $V^{(A)}$  has two turning points,  $x_L < x_R$ , so that

$$V^{(A)}(x_L) = V^{(A)}(x_R) = E \quad (17)$$

the function increasing monotonically beyond the turning points. Consider first the case when  $x_0 < x_L$ . It may be shown that bulk of the overlap integral is concentrated in the interval  $(x_0, x_L)$  where the wave functions behave for small  $\hbar$  as<sup>10</sup>

$$\psi^{(D)}(x) \approx \exp\left[-\frac{1}{\hbar} \int_{x_0}^x \mu^{(D)}(x') dx'\right] \quad (18)$$

$$\psi^{(A)}(x) \approx \exp\left[-\frac{1}{\hbar} \int_{x_L}^x \mu^{(A)}(x') dx'\right] \quad (19)$$

both functions are real, and

$$\mu^{(D)} = ip^{(D)}(x) = [2(v(x - x_0) - v_0)]^{1/2} \quad (20)$$

$$\mu^{(A)} = ip^{(A)}(x) = -[2(V^{(A)}(x) - E)]^{1/2} \quad (21)$$

are the classical momenta in the *inverted*<sup>8</sup> potentials. The overlap function  $\psi^{(D)}(x)\psi^{(A)}(x)$  has a sharp maximum at the point  $x = x_c$ , which is the point of crossing of the potentials,

$$V^{(D)}(x_c) - v_0 = V^{(A)}(x_c) - E \quad x_0 < x_c < x_L \quad (22)$$

The overlap integral is estimated at  $\hbar \rightarrow 0$  as in eq 15 with

$$w_L = \int_{x_0}^{x_c} \mu^{(D)}(x) dx + \int_{x_L}^{x_c} \mu^{(A)}(x) dx \quad (23)$$

The case when  $x_0 > x_R$  is considered in a similar way, giving

$$w_R = \int_{x_0}^{x_c} \mu^{(D)}(x) dx + \int_{x_R}^{x_c} \mu^{(A)}(x) dx \quad (24)$$

where  $\mu^{(D)}(x)$  and  $\mu^{(A)}(x)$  are defined as in eqs 20 and 21 but

with an opposite sign of the square root. In this way, we determine the overlap in cases when  $x_0 < x_L$ ,  $x_0 > x_R$ , and also in the interval  $(x_L, x_R)$  in the vicinities of the points  $x_L$  and  $x_R$  by analytic continuation of  $w_L$  and  $w_R$  as functions of the position of minimum of the donor potential  $x_0$ . These functions are zero at points  $x_0 = x_L$  and  $x_0 = x_R$  when the transition becomes classically allowed (without tunneling) and are analytic in the vicinity of these points. For example,  $w_L = \omega/2(x_L - x_0)^2 - [\omega^3/(6V_1)](x_L - x_0)^3 + O(x_L - x_0)^4$  where  $\omega = [v''(0)]^{1/2}$  and  $V_1 = V^{(A)}(x_L)$ . Finally, when  $x_0 \in (x_L, x_R)$ , we have found through many examples (but without deriving a general proof) that the overlap in this case may be determined by considering two analytic continuations with respect to the variable  $x_0$ , yielding

$$w = \min(\text{Re } w_L, \text{Re } w_R) \quad (25)$$

In section 4.4, we will need another form for  $w_L$  and  $w_R$  obtained by considering the crossing point  $x_c$  as a function of the position of the minimum  $x_0$  of  $V^{(D)}(x)$ . By differentiating eq 23 and taking into account that  $p^{(D)}(x_c) + p^{(A)}(x_c) = 0$ , we find  $dw_L/dx_0 = -p^{(D)}(qc)$ , so  $w_L$  can be rewritten in a more compact form as

$$w_L = -\int_{x_L}^{x_0} \mu_c(x'_0) dx'_0 \quad (26)$$

where

$$\mu_c(x'_0) = [2(v(x'_c - x'_0) - v_0)]^{1/2} \quad (27)$$

and  $x'_c$  is defined by the equation

$$v(x'_c - x'_0) - v_0 = V^{(A)}(x'_c) - E, \quad x'_0 < x'_c < x_R \quad (28)$$

$w_R$  can be written in a similar form.

#### 4. Jumping and Hopping in Phase Space

New insight can be gained by studying the Franck–Condon factors in the Wigner representation:

$$f_{D \rightarrow A} = 2\pi\hbar \int dx dp \rho^{(D)}(x,p) \rho^{(A)}(x,p) \quad (29)$$

where the Wigner function is defined by the transform

$$\rho(x,p) = \frac{1}{\pi\hbar} \int d\eta \exp\left(-\frac{2i}{\hbar}p\eta\right) \psi^*(x+\eta)\psi(x-\eta) \quad (30)$$

In the previous section, we determined the point  $x_c$  dominating the overlap integral in coordinate space by finding the stationary-phase point of the integrand and recognizing that it is the crossing point of the two potential energy surfaces. Hopping or jumping occurred at this coordinate with the momentum given by  $p_c = \sqrt{2m(E - V(x_c))}$ . The physical meaning of complex  $x_c$  and complex  $p_c$  is somewhat obscure.

Here, we define  $(x_m, p_m)$  to be the phase-space point dominating the phase-space overlap integral. The Wigner function is real so that we find  $(x_m, p_m)$  by finding the maximum of the phase-space integrand. As in coordinate space, there may be more than one maximum point, yet we shall assume that we are dealing with the dominant contribution. By definition,  $(x_m, p_m)$  are real and thus easily lend themselves to interpretation as the nuclear coordinates and momenta at the hopping or jumping point.

In previous publications, we have introduced this concept and demonstrated that it gives a useful interpretation.<sup>11,12</sup> First, we showed for a model that the jumping point found in this way

gives the correct initial conditions for dynamics on the accepting surface.<sup>12,13</sup> Second, we showed that in a multidimensional system, the specific nature of the jump singles out the coordinate system most appropriate for analyzing the jump. For example, for radiationless transitions, one can find in this way the dominant accepting mode(s).<sup>12,13</sup> Work is in progress to calculate overall transition rates (as contrasted with the above-mentioned relative phase-space propensities) in multidimensional systems. This may be accomplished by expanding the integrand around the jumping point.

The phase-space approach has several advantages over the traditional semiclassical methods. The phase-space picture of the jump trivially extends to any number of dimensions. One just has to find the multidimensional point in phase space that has the maximal value of the integrand of eq 29 with respect to each coordinate and momentum. Extension of the traditional semiclassical approach to many dimensions is much more difficult. The phase-space approach allows for both small hops between close surfaces and large jumps, say, between nested potential energy surfaces when it is impossible to hop.

While the power of the phase-space picture comes forth in multidimensional systems and for large jumps, we focus below on one-dimensional transitions between close surfaces. The examples that we consider are chosen so as to allow for a comparison between the two approaches in cases accessible to both. We hope to achieve two goals by doing so: first, to verify that the new approach reproduces correctly the results of the traditional methods and, second, to gain some insight as to the physical meaning of complex crossing points.

We have defined the point dominating the phase-space integral,  $(x_m, p_m)$ , as the “jumping point”—the point in phase space where the transition between the two potential energy surfaces occurs. Below, we focus on the relations between the more traditional hopping point  $x_c$  and our new definition for the jumping point at  $(x_m, p_m)$ . Instead of formally studying all possible cases, we focus on specific examples in which both  $x_c$  and  $(x_m, p_m)$  are well defined and show that for these examples

$$x_m \approx \text{Re } x_c \quad (31)$$

$$p_m \approx \text{Re } p_c = \pm \text{Re } \sqrt{2m(E - V(x_c))} \quad (32)$$

Equations 31 and 32 imply that in one dimension, and in the quasiclassical limit, the transitions occur at such jumping points so that the coordinate of the jump is equal to the real part of the generally complex crossing point of the two potential energy surfaces and the momentum of the jump is equal to the real part of the generally complex momentum at that crossing point. For the simplest case of real crossing in a classically allowed region, we get  $x_m \approx x_c$  and  $p_m \approx p_c$ . Real crossing in the classically forbidden region occurs with  $x_m \approx x_c$  and  $p_m \approx 0$  because  $p_c$  in these cases is purely imaginary.

There are strong analogies between looking for a point in complex coordinate space dominating the FC factor integral and looking for a point in real phase space dominating the same integral in a different representation. Both methods sample the same phase space. We note in passing that in both cases the number of real variables on which the search for a dominant point is carried out is twice the number of degrees of freedom. In the first, more traditional approach, the momentum  $p_c$  is calculated *after* the complex coordinate  $x_c$  is found. In the phase-space approach,  $x_m$  and  $p_m$  are found simultaneously yet are both real. Equations 31 and 32 make the connection between these two seemingly different pictures. Positions and momenta are related by Fourier transforms, and real and imaginary parts



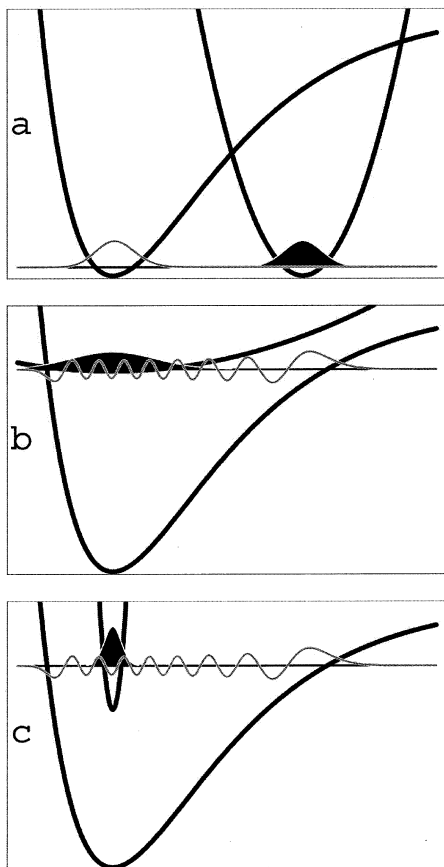


**Figure 2.** Three cases showing relative positions of minima and relative shapes of potential energy surfaces resulting in very different regimes of Franck–Condon overlap. In panel a, we show the overlap of two ground states leading to a position jump, in panel b, we show a case of a shallow donor potential leading to a position jump, and in panel c, we show nested potentials with a steep donor potential leading to a momentum jump.

of physical quantities are related by analyticity. We would like to assign physical significance to the jumping point, at least in the semiclassical limit and for cases in which the jumping point is well defined. It is difficult to assign physical meaning to a complex coordinate. Equations 31 and 32, when they apply, assign such physical meaning to  $x_c$  through the following prescription: one must calculate  $p_c$  from  $x_c$  and then take the real parts of both. This gives the physical coordinates and momenta of the transition between the potential surfaces.

We now proceed to justify eqs 31 and 32. We would like to find the jumping point ( $x_m, p_m$ ) that is the extremum point of the integrand in eq 29. In section 5, we do so numerically for some examples. Here, we take an analytic approach that requires that we first find some explicit form for the Wigner functions,  $\rho^{(D)}(x,p)$  and  $\rho^{(A)}(x,p)$ . We do so for the examples depicted in Figure 2.

**4.1. Quasiclassical Approximation for the Donor Wigner Function,  $\rho^{(D)}(x,p)$ .** Let the initial state be the ground vibrational state of the donor potential energy surface so that the wave function is given by eq 13. The classically forbidden region is the entire real axis except for the region between the two classical turning points. Most of the cases that we consider are dominated by the region where eq 13 is valid, in the deeply forbidden region. Note that under these assumptions,  $\sigma(x)$  is real for real  $x$ .

Using the definition of the Wigner function (eq 30) and the quasiclassical formula (eq 13), we express the Wigner function

of the donor state as

$$\rho(x,p) = \frac{1}{\pi\hbar} \int d\eta C_\psi(x+\eta)C_\psi(x-\eta) \exp\left(-2\frac{i}{\hbar}\Phi\right) \quad (33)$$

where  $C_\psi(x)$  is the (real) preexponential part of the wave function and

$$\Phi = \frac{1}{2i}[\sigma(x+\eta) + \sigma(x-\eta)] + p\eta \quad (34)$$

We consider the integral in the complex  $\eta$  plane, applying analytic continuation. In the quasiclassical limit, the dominant contributions to the integral (eq 33) come from those values of  $\eta = \eta_s$  for which the exponent is stationary, that is, where

$$\partial\Phi/\partial\eta = \frac{1}{2i}[\sigma'(x+\eta) - \sigma'(x-\eta)] + p = 0 \quad (35)$$

Equation 35 implies

$$\text{Re } \sigma'(x+\eta_s) = \text{Re } \sigma'(x-\eta_s) \quad (36)$$

$$\text{Im } \sigma'(x+\eta_s) - \text{Im } \sigma'(x-\eta_s) + 2p = 0 \quad (37)$$

These equations can be solved assuming that  $\eta_s$  is purely imaginary. We conjecture here that this solution gives the dominant contribution. Then, because the function  $\sigma$  is real for real arguments and because  $p$  and  $x$  are real, eq 35 for the stationary point is simplified further as

$$\text{Im } \sigma'(x+\eta_s) + p = 0 \quad (38)$$

Finally, the integral (eq 33) is estimated as

$$\rho(x,p) \approx \exp\left(-\frac{2}{\hbar}W(x,p)\right) \quad (39)$$

$$W(x,p) = i\Phi|_{\eta=\eta_s} = \text{Re } \sigma(x+\eta_s) + ip\eta_s \quad (40)$$

*Wigner Function for Harmonic and Anharmonic Oscillators.* As an example of the utility of the analysis above, let us consider a harmonic oscillator perturbed by cubic anharmonicity,

$$H(x,p) = \frac{1}{2}p^2 + \frac{1}{2}\omega^2x^2 + \frac{1}{6}\lambda x^3 \quad (41)$$

where the parameter  $\lambda$  is small.

The function  $\sigma'(x)$  is the same as the classical momentum in the inverted potential. By integration, we find  $\sigma(x) = \omega x^2/2 + \lambda x^3/(18\omega)$  (neglecting terms of order  $\lambda^2$ ). By solving eq 38, we get  $\eta_s = -ip/\omega + i\lambda xp/(3\omega^3)$  and

$$W = \frac{1}{2}\omega x^2 + \frac{1}{2\omega}p^2 + \frac{\lambda}{6\omega}\left(\frac{x^3}{3} - \frac{xp^2}{\omega^2}\right) \quad (42)$$

The first two terms in eq 42

$$W_0 = \frac{1}{2}\omega x^2 + \frac{1}{2\omega}p^2 \quad (43)$$

give the exact function  $W$  for the harmonic oscillator, and the third term is the first anharmonic correction in the quasiclassical limit. In ref 13, the Wigner function of anharmonic potentials was derived for a more general multidimensional case and without taking the quasiclassical limit. Equations 67 and 70 from ref 13 reduce to eq 42 by taking  $\hbar \rightarrow 0$ .

**4.2. Quasiclassical Approximations for the Acceptor Wigner Function  $\rho^{(A)}(x,p)$ .** We consider two different approximations for the acceptor Wigner function,  $\rho^{(A)}(x,p)$ . If the final state is the ground state of the acceptor potential energy surface, it is best approximated by eq 40. If, on the other hand, it is some excited vibrational state or, as is often the case, a manifold of degenerate excited states, a useful approximation gives

$$\rho^{(A)}(x,p) \approx \delta(H^{(A)}(x,p) - E) \quad (44)$$

Equation 44 was derived in ref 14 for the more general case of a potential of several variables. It is known to be the first term in a power series in  $\hbar$ .<sup>14,15</sup> In fact, in the quasiclassical limit,

$$\rho_E^{(A)}(x,p) = \frac{1}{2\pi} \delta(H^{(A)}(x,p) - E) \quad (45)$$

if the final state is given by the microcanonical density matrix, and

$$\rho_{\text{pure}}^{(A)}(x,p) = \frac{1}{2\pi} [D^{(A)}(E)]^{-1} \delta(H^{(A)}(x,p) - E) \quad (46)$$

for a pure state. In one dimension, eq 46 can also be derived by approximating the Wigner function of the final state by its classical ( $p = 0$ ) limit as<sup>16</sup>

$$\rho_{\text{pure}}^{(A)}(q,p) = \frac{1}{2\pi} \delta(I(x,p) - n) \quad (47)$$

where  $n = 0, 1, 2, \dots$  is the quantum number of the final state and

$$I(x,p) = \frac{1}{2\pi} \oint_{H^{(A)}(x',p')=H^{(A)}(x,p)} p' dx' \quad (48)$$

Changing the argument of the  $\delta$ -function, eq 47 is rewritten as eq 46 where  $D^{(A)}(E)$  is the density of states at energy  $E$ . Note that  $\rho_E^{(A)} = D^{(A)}(E) \rho_{\text{pure}}^{(A)}$ .

**4.3. Quasiclassical Estimation of the Franck–Condon Factor for Transitions between Two Ground States.** Let both donor and acceptor states be the ground states, each on its respective potential energy surface. In this case

$$\begin{aligned} \rho^{(D)}(x,p) &\approx \exp\left(-\frac{2}{\hbar} W^{(D)}(x,p)\right) \\ W^{(D)}(x,p) &= \text{Re } \sigma^{(D)}(x + \eta_s^{(D)}) + i p \eta_s^{(D)} \\ \rho^{(A)}(x,p) &\approx \exp\left(-\frac{2}{\hbar} W^{(A)}(x,p)\right) \\ W^{(A)}(x,p) &= \text{Re } \sigma^{(A)}(x + \eta_c^{(A)}) + i p \eta_c^{(A)} \end{aligned} \quad (49)$$

The Franck–Condon factor of eq 29 is then given by

$$f = \frac{1}{\pi \hbar} \int dx dp C_\rho^{(D)}(x,p) C_\rho^{(A)}(x,p) \exp\left(-\frac{2}{\hbar} \Theta\right) \quad (50)$$

where  $C_\rho(x,p)$  is the preexponential part of the Wigner function and

$$\Theta = \text{Re } \sigma^{(D)}(x + \eta_s^{(D)}) + i p \eta_s^{(D)} + \text{Re } \sigma^{(A)}(x + \eta_c^{(A)}) + i p \eta_c^{(A)} \quad (51)$$

In the limit of  $\hbar \rightarrow 0$  the dominant contributions to the integral (eq 50) come from those values of  $x = x_m$  and  $p = p_m$  for which

the exponent is maximal with respect to both  $x$  and  $p$ , that is, where

$$\frac{d\Theta}{dx} = \text{Re } \sigma^{(D)'}(x + \eta_s^{(D)}) + \text{Re } \sigma^{(A)'}(x + \eta_s^{(A)}) = 0 \quad (52)$$

$$\frac{d\Theta}{dp} = i \eta_s^{(D)} + i \eta_s^{(A)} = 0 \quad (53)$$

Denoting  $\eta_s = \eta_s^{(D)} = -\eta_s^{(A)}$ , we rewrite eq 52 as

$$\text{Re } \sigma^{(D)'}(x_m + \eta_s) + \text{Re } \sigma^{(A)'}(x_m - \eta_s) = 0 \quad (54)$$

Eliminating  $p$  from two eqs 38, one for the initial and another for the final state, we have

$$\text{Im } \sigma^{(D)'}(x_m + \eta_s) - \text{Im } \sigma^{(A)'}(x_m - \eta_s) = 0 \quad (55)$$

Finally, combining together eqs 54 and 55 and taking into account that  $\text{Re } \sigma^{(A)'}(x_m - \eta_s) = \text{Re } \sigma^{(A)'}(x_m + \eta_s)$  and  $\text{Im } \sigma^{(A)'}(x_m - \eta_s) = -\text{Im } \sigma^{(A)'}(x_m + \eta_s)$ , we get

$$\sigma^{(D)'}(x_m + \eta_s) + \sigma^{(A)'}(x_m + \eta_s) = 0 \quad (56)$$

Introducing  $p_c$  as the solution of the equation  $H^{(D)}(x_c, p_c) = E$ , it follows from eq 14 that  $p_c = S^{(D)'}(x_c) = i \sigma^{(D)'}(x_c)$  and similarly  $p_c = S^{(A)'}(x_c) = i \sigma^{(A)'}(x_c)$ . Comparing eq 56 with the equation  $p^{(D)}(x_c) + p^{(A)}(x_c) = 0$ , we see that  $x_m + \eta_s$  is the complex coordinate of crossing of the potentials  $V^{(D)}$  and  $V^{(A)}$  and

$$x_c = x_m + \eta_s \quad (57)$$

Finally, using the facts that  $x_m$  is real and  $\eta_s$  is purely imaginary and applying eq 38, we establish that

$$x_m = \text{Re } x_c \quad (58)$$

$$p_m = -\text{Im } \sigma^{(D)'}(x_c) = \text{Re } p_c \quad (59)$$

**4.4. Transitions between the Ground Vibrational State of the Donor Potential Energy Surface and a Manifold of Vibrationally Excited States of the Acceptor Potential Energy Surface.** Let the donor state be the ground state on its potential energy surface and the acceptor state be an excited vibrational state or a manifold of degenerate excited states. In this case,

$$\begin{aligned} \rho^{(D)}(x,p) &\approx \exp\left(-\frac{2}{\hbar} W^{(D)}(x,p)\right) \\ W^{(D)}(x,p) &= \text{Re } \sigma^{(D)}(x + \eta_s^{(D)}) + i p \eta_s^{(D)} \\ \rho^{(A)}(x,p) &= \delta(H^{(A)}(x,p) - E) \end{aligned} \quad (60)$$

This approximation is not restricted to the ground state.

The Franck–Condon factor (eq 29) is then roughly (without a prefactor) expressed as

$$f \approx \exp\left(-\frac{2}{\hbar} W_m\right) \quad (61)$$

where  $W_m = W^{(D)}(x_m, p_m)$  is the minimum value of  $W^{(D)}$  on the surface of constant energy,  $H^{(A)}(x,p) = E$ . The logarithm of the Franck–Condon factor  $W_m$  depends on both potential energy surfaces and on the energy gap, because it is a constrained minimum of a function defined on the donor potential energy surface where the constraint is defined by the acceptor potential energy surface and the energy.

Note that we define the “jumping point”  $(x_m, p_m)$  as the point where the integrand of the phase-space overlap integral is maximal. This notation is the same as that in section 4.3, although, in general, the two points need not be the same because they are the extremum points of different approximations for the integrand.

Let us establish the relation between the jumping point  $(x_m, p_m)$  of eq 61 and the crossing point of the potential energy surfaces  $(x_c, p_c)$  and between the logarithm of the Franck–Condon factor  $w$  as calculated in section 3 within the traditional approach and the logarithm of the Franck–Condon factor  $W_m$  as calculated here within the phase-space approach. We restrict ourselves to two cases, the case when the potential  $V^{(D)}$  is shallow or that when it is a steep function in comparison with the function  $V^{(A)}$ . We show below that in these limiting cases eqs 31 and 32 hold and in addition  $W_m = w$ . The phase-space approach agrees then with the traditional semiclassical method of section 3 above.

**Shallow Minimum Potential  $V^{(D)}$ .** For a shallow minimum potential when  $V^{(D)} \approx v_0$ , the turning point and the crossing point,  $x_R$  and  $x_c$  defined by eqs 17 and 22, almost coincide,  $x_R \approx x_c$ , so that the method of section 3 gives for the logarithm of the Franck–Condon factor

$$w = w_R \approx \int_{x_0}^{x_R} \mu^{(D)}(x) dx \quad (62)$$

where  $\mu^{(D)}$  was defined in eq 20 and we assume for definiteness that the transition goes through the right turning point, that is,  $w_L > w_R$ .

Now, let us consider this case within the phase-space formalism of eq 61. First, we prove that, if  $V^{(D)} \approx v_0$  and the action  $\sigma^{(D)}(x)$  is small, then only a coordinate jump is possible. For small momenta, eq 38 is solved by  $\eta_s = -ip/\sigma''(x)$ . Substituting it in eq 40, we find that

$$W(x, p) \approx \sigma(x) + \frac{1}{2} \frac{p^2}{\sigma''(x)} \quad (63)$$

Under the assumption regarding the shape of the function  $v(x)$  in eq 16 (see the beginning of subsection 3.3), we have  $\sigma^{(D)''}(x) > 0$ . Now, it follows from eq 63 that the function  $W(x, p)$  is small at  $p = 0$  and rapidly increases when the momentum becomes nonzero. For such a function, it is obvious that its minimum occurs at  $p_m = 0$  (no momentum jump).

We suppose here that the potential of the acceptor is steeper on the right side, so that  $W^{(D)}(x_R, 0) < W^{(D)}(x_L, 0)$ , and we conclude that

$$x_m = x_R \approx x_c \quad (64)$$

$$p_m = 0 = \text{Re } p_c \quad (65)$$

$$W_m = w = \sigma^{(D)}(x_R) \quad (66)$$

This means that the result of the phase-space approach is the same as the quasiclassical result when the overlap is approximated by an exponent of the action  $\sigma(x_R)$ .

**Steep Potential  $V^{(D)}$ .** Consider the opposite case of a steep donor potential  $V^{(D)}$ . Here too, we would like to compare the results of the more traditional analysis in coordinate space with the phase-space analysis.

First, following section 3, we look for  $x_c$ , the point of crossing of the two potential energy surfaces, and the Franck–Condon factor as given by eq 15. We approximate the donor potential  $V^{(D)}$  near its minimum as

$$V^{(D)}(x) \approx v_0 + \frac{\omega^{(D)^2}}{2}(x - x_0)^2 + \dots \quad (67)$$

where the frequency  $\omega^{(D)}$  is supposed to be large. We find the crossing point of the potentials by an expansion of  $V^{(A)}$  in a Taylor series around the point  $x_0$ ,

$$V^{(A)}(x) \approx V^{(A)}(x_0) + V^{(A)'}(x_0)(x - x_0) + \dots \quad (68)$$

and by solving eq 22. The result is

$$x_c \approx x_0 \pm \frac{i}{\omega^{(D)}} \{2[E - V^{(A)}(x_0)]\}^{1/2} + \frac{V^{(A)'}(x_0)}{\omega^{(D)^2}} \quad (69)$$

(we consider here only “nested” potentials when the square root in eq 69 is real). The momentum at the crossing point is

$$p_c = i\mu_c^{(D)} \approx \pm \{2[E - V^{(A)}(x_0)]\}^{1/2} + i \frac{V^{(A)'}(x_0)}{\omega^{(D)}} \quad (70)$$

Using eqs 70 and 26, we estimate

$$\begin{aligned} \text{Re } w_L &= \int_{x_0}^{x_L} \text{Re } \mu_c(x'_0) dx'_0 \\ &\approx \frac{1}{\omega^{(D)}} \int_{x_0}^{x_L} V^{(A)'}(x'_0) dx'_0 = \frac{E - v_0}{\omega^{(D)}} \end{aligned} \quad (71)$$

Estimation of  $\text{Re } w_R$  is the same. Using eq 25, we find

$$w \approx \frac{E - v_0}{\omega^{(D)}} \quad (72)$$

The phase-space approach reproduces eq 71 straightforwardly. In the harmonic approximation, the Wigner function is given by eq 43. When the frequency is large, the coordinates of the jumping point satisfying  $H^{(A)} = E$  and reducing  $W_0$  to a minimum are  $x_m = x_0$  and  $p_m = [2(E - v_0)]^{1/2}$ , so  $W_m = (E - v_0)/\omega^{(D)}$ . Finally, notice that from eq 69 it follows that  $x_m \approx \text{Re } x_c$  and from eq 70 it follows that  $p_m \approx \pm \text{Re } p_c$ . The plus–minus sign appears because of the existence of two equivalent jumping points.

## 5. Numerical Examples

Let us consider an example of the harmonic potential of the donor

$$V^{(D)}(x) = \frac{1}{2} \omega^2 x^2 \quad (73)$$

and either Morse potential

$$V^{(A)}(x) = \frac{1}{2} \left( J + \frac{1}{2} \right) (1 - e^{-\beta x})^2, \quad \beta = \left( J + \frac{1}{2} \right)^{-1/2}, \quad J = 300 \quad (74)$$

or Poeschl–Teller potential

$$V^{(A)}(x) = \frac{1}{2} \alpha^{-2} (\cosh^{-2} \alpha x - 1), \quad \alpha = [J(J + 1)]^{-1/4}, \quad J = 400 \quad (75)$$

of the acceptor. There are in total  $J$  bound states in potentials 74 and 75 labeled by quantum numbers  $n = 0, 1, 2, \dots, J - 1$ . In the case of Morse potential, we consider the excited state with the quantum number  $n = 150$  and energy  $E = 112.812$

**TABLE 1: Numerical Results for Various Frequencies  $\omega$  of the Donor Potential (Eq 73) and for Two Options for the Acceptor Potential, Either Morse (M) or Poeschl–Teller (PT), Eqs 74 and 75<sup>a</sup>**

$\omega$	$V^{(A)}$	$x_c$	$p_c$	$x_m$	$p_m$	$w_c$	$W_m$	$w$	case
0.2	M	−10.90	2.18i	−10.82	0	11.8	11.7	14.1	shallow $V^{(D)}(x)$
1.0	M	−13.34	13.34i	−10.82	0	67.6	58.5	69.5	
1.3	M	−15.56	20.22i	−10.82	0	98.6	76.1	100.6	
5.0	M	0.01 − 3.06i	−15.32 − 0.06i	0	−15.02	22.9	22.6	24.4	steep $V^{(D)}(x)$
0.2	PT	32.52	6.50i	26.38	0	77.9	69.6	78.1	shallow $V^{(D)}(x)$
0.5	PT	21.95 + 15.62i	−7.81 + 10.97i	22.44	−6.25	176.2	165.0	177.6	
1.0	PT	12.10 + 16.49i	−16.49 + 12.10i	0	−17.34	179.6	150.3	180.2	
5.0	PT	3.54i	−17.70	0	−17.34	30.5	30.1	31.9	steep $V^{(D)}(x)$

<sup>a</sup>  $x_c$ , defined by the equation  $V^{(D)}(x_c) - v_0 = V^{(A)}(x_c) - E$ , is the coordinate where potentials cross, and  $p_c = \pm[2(v_0 - V^{(D)}(x_c))]^{1/2} = \pm i\omega x_c$  is the momentum at the crossing point.  $(x_m, p_m)$  is the point in phase space on the surface of constant energy  $H^{(A)}(x, p) = E$  where the Wigner function,  $\rho^{(D)}(x, p)$ , reaches its maximum.  $w = -(\hbar/2) \ln f_{D \rightarrow A}$  is proportional to the logarithm of the Franck–Condon factor;  $w_c$  and  $W_m$  are, respectively, the quasiclassical and phase space approximations to  $w$ , see sections 3.3 and 4.4. In the cases of several equivalent jumping points, we give only one of them.

and in the case of Poeschl–Teller potential the quantum number  $n = 200$  and energy  $E = 150.312$ .

If the parameter  $\omega$  is small, the donor potential is relatively shallow, and when it is large,  $V^{(D)}(x)$  is steep. Numerical results are shown in Table 1. A similar table was generated for an earlier paper, but the parameters and the comparisons being made were somewhat different.<sup>11</sup> For cases of steep or shallow potential  $V^{(D)}(x)$ , relations 58 and 59 are satisfied with good accuracy.

## 6. Summary and Conclusions

The trajectory surface hopping methods initiated by the famous Tully and Preston paper<sup>1</sup> have been widely applied in chemistry.<sup>17</sup> In this paper, we have provided perspective, new analysis, and testing of nonstandard approaches to surface hopping and jumping. For the cases of surface hopping in one or many dimensions or surface jumping in one dimension, the techniques that we discuss are simply instructive alternatives to other approaches. Our intent in these cases has been to compare the various techniques with the Wigner phase-space approach, because only the latter generalizes easily to many dimensions. We have been able to give a rather more solid grounding to the Wigner phase-space surface jumping method<sup>11–13</sup> than had been the case previously, especially through the semiclassical analysis with complex stationary phase. It is our belief that for cases of slow radiationless transition or in the wings of absorption bands (where again FC factors are very unfavorable and correspond to tunneling events because there is no nearby crossing of potential energy surfaces) that the phase-space approach may be the only viable way to do calculations of relative rates and of promoting and accepting modes. At the same time, the phase-space “surface jumping” approach is a very intuitive one, providing clear pictures of the mechanism for radiationless or nonvertical radiative transitions in terms of bond length changes or bond momentum jumps or both in one or more coordinates.

It may be interesting to combine the generalization of hops into jumps with some new developments in mixed quantum–classical Liouville propagation recently introduced by Ciccotti et al. and Martens et al.<sup>18–22</sup> These two approaches and our phase-space surface jumping approach seem to complement each other in several ways. In the formalism of refs 19–21, for example, for the specific case of nonradiative nonadiabatic processes, the excess energy flows in the direction of the nonadiabatic coupling vector and is dumped into the velocities. The phase-space approach provides a systematic way for predicting the energy flow during a transition between non-crossing surfaces. We have recently found, within the phase-

space analysis, that for small energy gaps between the surfaces (as in hopping) the excess energy flows in the direction of the nonadiabatic coupling vector, but we have also found that this rule does not apply in general to large energy gaps.<sup>23</sup> In the general case, the jump is sensitive to the shape of the accepting potential and to the initial distribution on the donor surface. This sensitivity can sometimes reduce in principle the number of trajectories one needs to consider, yet it requires some sampling of phase space to determine the relevant jumps. So far, the phase-space approach does not take into account interference from different jumps, although it is clear that such interferences could be important, in particular, between two momentum jumps of opposite signs. Future work could consider combining the treatment of coherences as in ref 18 with the phase-space jumping mechanism to properly account for interference.

**Acknowledgment.** This research was supported by a grant (2000118) from the United States–Israel Binational Science Foundation (BSF), Jerusalem, Israel.

## References and Notes

- (1) Tully, J. C.; Preston, R. K. *J. Chem. Phys.* **1971**, *55*, 562.
- (2) Nikitin, E. F. *Theory Elementary Atomic and Molecular Processes in Gases*; Clarendon: Oxford, U.K., 1974.
- (3) Avouris, P.; Gelbart, W. M.; El-Sayed, M. A. *Chem. Rev.* **1977**, *77*, 793.
- (4) Ewing, G. J. *Phys. Chem.* **1987**, *91*, 4662.
- (5) Bergsma, J. P.; Behrens, P. H.; Wilson, K. R.; Fredkin, D. R.; Heller, E. J. *J. Phys. Chem.* **1984**, *88*, 612.
- (6) Medvedev, E. S. *Chem. Phys.* **1982**, *73*, 243–251.
- (7) Hunt, P. M.; Child, M. S. *Chem. Phys. Lett.* **1978**, *58*, 202.
- (8) Miller, W. H. *Adv. Chem. Phys.* **1974**, *XXV*, 69.
- (9) Berry, M. V. *Proc. R. Soc. London, Ser. A* **1977**, *287*, 237.
- (10) Landau, L. D.; Lifshitz, E. M. *Quantum Mechanics: Non-Relativistic Theory*; Pergamon: Oxford, U.K., 1977.
- (11) Heller, E. J.; Beck, D. *Chem. Phys. Lett.* **1993**, *202*, 350.
- (12) Segev, B.; Heller, E. J. *J. Chem. Phys.* **2000**, *112*, 4004.
- (13) Sergeev, A. V.; Segev, B. *J. Phys. A: Math. Gen.* **2002**, *35*, 1769.
- (14) Heller, E. J. *J. Chem. Phys.* **1978**, *68*, 2066.
- (15) Hüpper, B.; Eckardt, B. *Phys. Rev. A* **1998**, *57*, 1536.
- (16) Berry, R. S.; Nielsen, S. E. *Phys. Rev. A* **1970**, *1*, 383.
- (17) Tully, J. C. In *Modern Methods for Multidimensional Dynamics Computations in Chemistry*; Thompson, D. L., Ed.; World Scientific: Singapore, 1998; p 34.
- (18) Donoso, A.; Martens, C. C. *J. Phys. Chem. A* **1998**, *102*, 4291.
- (19) Kapral, R.; Ciccotti, G. *J. Chem. Phys.* **1999**, *110*, 8919.
- (20) Neilsen, S.; Kapral, R.; Ciccotti, G. *J. Chem. Phys.* **2000**, *112*, 6543.
- (21) Neilsen, S.; Kapral, R.; Ciccotti, G. *J. Chem. Phys.* **2001**, *115*, 5805.
- (22) Donoso, A.; Martens, C. C. *Phys. Rev. Lett.* **2001**, *87*, 223202–1.
- (23) Kallush, S.; Segev, B.; Sergeev, A. V.; Heller, E. J. *J. Phys. Chem. A*, in press.